Proc. Natl. Acad. Sci. USA
Vol. 96, pp. 3836–3841, March 1999
Genetics

Genetic analysis of the mouse X inactivation center defines an 80-kb multifunction domain

JEANNIE T. LEE*†‡, NAIFUNG LU*, AND YOON HAN*

*Department of Molecular Biology, Massachusetts General Hospital, and †Department of Genetics, Harvard Medical School, Boston, MA 02114

Communicated by Shirley M. Tilghman, Princeton University, Princeton, NJ, January 20, 1999 (received for review December 8, 1998)

ABSTRACT **Dosage compensation in mammals occurs by X inactivation, a silencing mechanism regulated in cis by the X inactivation center (*Xic*). In response to developmental cues, the *Xic* orchestrates events of X inactivation, including chromosome counting and choice, initiation, spread, and establishment of silencing. It remains unclear what elements make up the *Xic*. We previously showed that the *Xic* is contained within a 450-kb sequence that includes *Xist*, an RNA-encoding gene required for X inactivation. To characterize the *Xic* further, we performed deletional analysis across the 450-kb region by yeast-artificial-chromosome fragmentation and phage P1 cloning. We tested *Xic* deletions for cis inactivation potential by using a transgene (Tg)-based approach and found that an 80-kb subregion also enacted somatic X inactivation on autosomes. *Xist* RNA coated the autosome but skipped the *Xic* Tg, raising the possibility that X chromosome domains escape inactivation by excluding *Xist* RNA binding. The autosomes became late-replicating and hypoacetylated on histone H4. A deletion of the *Xist* 5′ sequence resulted in the loss of somatic X inactivation without abolishing *Xist* expression in undifferentiated cells. Thus, *Xist* expression in undifferentiated cells can be separated genetically from somatic silencing. Analysis of multiple *Xic* constructs and insertion sites indicated that long-range *Xic* effects can be generalized to different autosomes, thereby supporting the feasibility of a Tg-based approach for studying X inactivation.**

In mammals, dosage compensation is carried out by X inactivation in female cells (1). X inactivation is a multistep process that includes X chromosome counting, choice between X chromosomes for inactivation, initiation of silencing on the future inactive X (X_i), propagation of silent chromatin on that X, and establishment of X heterochromatin (2). Dosage compensation ensures that one X is kept active for each diploid autosomal set and all other X chromosomes are converted to heterochromatin. The X_i is hypermethylated (3), late-replicating (4), and hypoacetylated on core histone tails (5). The different steps of X inactivation are controlled by the X inactivation center (*Xic*), an X linked locus defined by X-to-autosome translocations (6). *Xist* remains the only *Xic* gene known to be required for X inactivation. *Xist* encodes a 15-kb untranslated RNA that is expressed only from the X_i and coats the chromosome in cis (7–9).

Transgene (Tg)-based assays in mouse embryonic stem (ES) cells have facilitated genetic analysis of the *Xic*. These assays are based on the fact that ES cells also enact X inactivation on induction of differentiation (10) and that autosomes can be inactivated when *Xic* sequences are present in cis (11, 12). Tg studies showed that the *Xic* is contained within a 450-kb sequence that includes *Xist* (11, 12). It has also been shown that a 35-kb cosmid carrying *Xist* with 9 kb of upstream and 6 kb of downstream sequence could express *Xist* in differentiating ES cells (13). However, it is not known whether the cosmid was sufficient for *Xist* expression and cis inactivation in somatic cells. Thus, the question of how much sequence comprises the minimal *Xic* remains to be addressed. Some suggest that the *Xic* is *Xist* itself (13, 14), but knockout studies implicate additional cis elements. Although *Xist* knockouts destroyed cis silencing, they did not abolish chromosome counting and choice, suggesting that these elements are separately encoded (9, 15). Moreover, deleting a 65-kb sequence downstream of *Xist* resulted in constitutive *Xist* expression, suggesting that regulatory elements lie downstream of *Xist* (16).

For this study, to characterize the *Xic*, we performed deletional analysis of the 450-kb murine *Xic* sequence and showed that X inactivation can be recapitulated by an 80-kb multifunction domain.

MATERIALS AND METHODS

Construction of *Xic* Deletions. Yeast-artificial-chromosome (YAC) fragmentation (17) was used to create large deletions by homologous recombination at B1 repeats in the 450-kb *Xic* YAC, Y116 (Fig. 1*A*; ref. 11). Acentric fragmentation vectors were created with the B1 repeat in two orientations (pfragF and pfragR; Fig. 1*B*). Homologous targeting of random B1 elements on the YAC created a series of incremental deletions. Y116 (11) was used for deleting sequences upstream of *Xist*. yJL29 was used for downstream deletions and was derived from a C57BL/6 library (Fig. 1*C*; ref. 18). Differing from Y116 in insert orientation, yJL29 circumvented the need to construct centric vectors, for which selection is difficult because they yield centric recombinants. Vectors were linearized at *Sal*I and transformed into Y116 and yJL29 cells. Only 7 of >100 *Xist*-containing recombinants were analyzed further. We also isolated three 80- to 85-kb clones (Fig. 1*D*) from a phage P1 library (Genome Systems, St. Louis). πJL1 carries 30 kb of sequence upstream of *Xist* and 30 kb of sequence downstream of *Xist*; πJL2 carries 30 kb of sequence upstream of *Xist* and 35 kb of sequence downstream of *Xist*; πJL3 carries a complete *Xist* structural gene with 730 bp of upstream sequence and 60 kb of downstream sequence. Thus, πJL3 contains the P_1 *Xist* promoter but lacks P_0 (proposed as an alternate *Xist* promoter; ref. 19). Long-range restriction maps were constructed by pulsed-field gel electrophoresis analysis and PCR mapping with microsatellite markers. Intact clones were used in this study.

Generation of Tg ES Cells and Fibroblasts. YAC DNA was introduced into J1 male ES cells (20) as described (21). P1 DNA was colipofected at a 10-fold molar excess relative to a *Neo* plasmid, and 10–40 independent Tg lines were generated for each YAC and P1 clone (Table 1). Tg integrity was assessed by Southern blot and densitometric analysis. Clones carrying stoichiometric ratios of vector and *Xist* sequences were considered intact. Fluorescence *in situ* hybridization (FISH) was used to

The publication costs of this article were defrayed in part by page charge payment. This article must therefore be hereby marked "*advertisement*" in accordance with 18 U.S.C. §1734 solely to indicate this fact.

PNAS is available online at www.pnas.org.

Abbreviations: Ch*n*; chromosome *n*; dapi, 4′,6-diamidino-2-phenylindole; EB, embryoid body; ES, embryonic stem; FISH, fluorescence *in situ* hybridization; Tg, transgene or transgenic; X_i, inactive X; *Xic*, X inactivation center; YAC, yeast artificial chromosome.

‡To whom reprint requests should be addressed. e-mail: lee@molbio.mgh.harvard.edu.

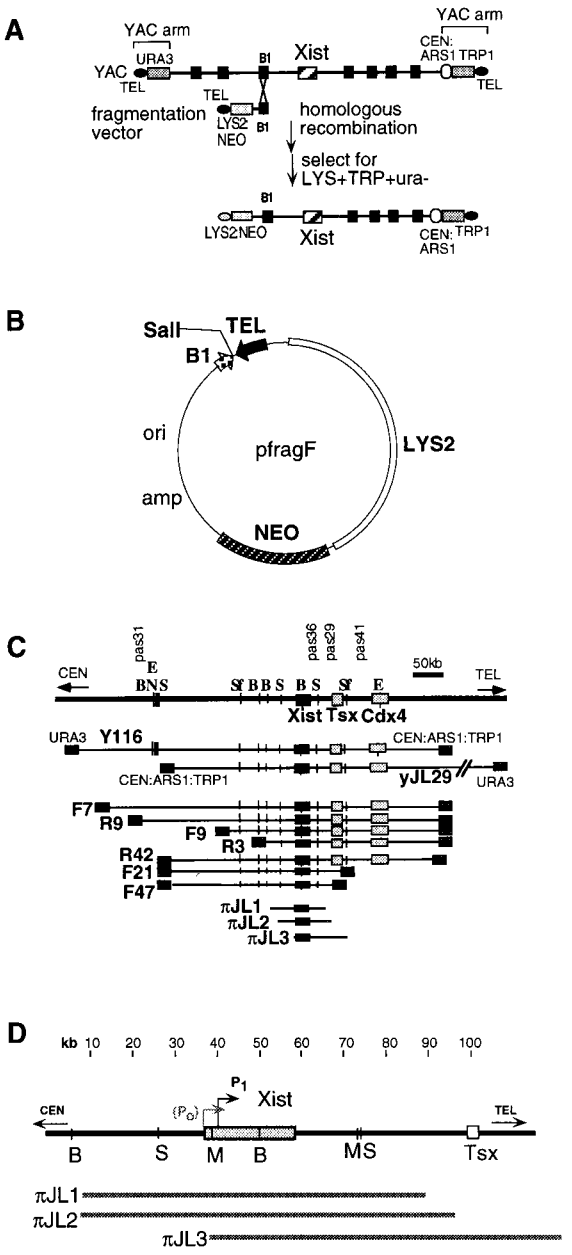

FIG. 1. YAC fragmentation scheme (*A*) and vector (*B*). (*C*) *Xic* deletion panel. E, *Eag*I; N, *Not*I; B, *Bss*HII; S, *Sal*I; Sf, *Sfi*I. (*D*) Map of P_1 clones.

identify insertion sites (Table 1). In multicopy integrations, all copies inserted at a single site. The line N1.1 was derived from a fragmented Y116 clone that lacked *Xist.* Chimeric mice were generated, and mixed fibroblasts were isolated from adults or day 13.5 embryos. Tg fibroblasts were cloned by limiting dilution after simian virus 40-large T immortalization (11) and were identified by PCR.

FISH. Detailed procedures have been described (22, 23). To detect RNA alone, cells were not denatured before hybridization. For simultaneous RNA/DNA FISH, samples were denatured, and large (100- to 500-kb) probes were used for DNA detection, together with small (2- to 5-kb) probes for RNA detection. Small probes allowed detection of multiple targets (RNA) but not single copy targets (DNA). *Xist* RNA was detected by exon 6 strand-specific probes (Promega pGEM single-stranded phage DNA system). Mouse chromosome paints were obtained from Oncor. *Xic* DNA was detected by Y116 or πJL3 probes. The X specific 250-kb bacterial artificial chromosome-*Zfx* probe has been described (11). Tg-specific hybridization was performed with P1 or YAC vector probes.

Table 1. Characteristics of *Xic* Tg lines

Xic derivative, size	Tg ES line	Tg copy no.	Integration site (chromosome)
F7, 400 kb	F7.14	Med	4
	F7.26	Med	Med. autosome
	F7.32	Low	17
F9, 250 kb	F9.3	Low	X
	F9.8	Low	8
	F9.18	Med	Large autosome
R3, 200 kb	R3.1	Low	Large autosome
	R3.3	Low	8
	R3.6	Low	8
R9, 325 kb	R9.3	Low	Med. autosome
	R9.5	Med	3
	R9.11	High	Small autosome
F21, 175 kb	F21.4	High	ND
	F21.18	Med	ND
	F21.21	High	ND
F47, 150 kb	F47.2	Med	ND
	F47.4	Med	ND
	F47.5	Med	ND
R42, 400 kb	R42.5	Low	ND
	R42.19	Low	ND
	R42.22	Low	ND
πJL1, 80 kb	πJL1.3	High	13
	πJL1.4	High	3
	πJL1.5	Med	3
πJL2, 85 kb	πJL2.4	High	10
	πJL2.5	High	8
	πJL2.7	High	Small autosome
πJL3, 80 kb	πJL3.6	High	2
	πJL3.8	High	X
	πJL3.10	High	10
N1	N1.1	Med	ND

Copy numbers are grouped into low (2–4), medium (5–9), and high (>10). ND, not determined. F7, F9, R3, and R9 are derived from Y116; F21, F47, and R42 are from yJL29.

Analysis of DNA Replication Timing and Histone H4 Acetylation. These assays were performed as described (5). Polyclonal antiacetylated H4 antibodies were obtained from Upstate Biotechnology (Lake Placid, NY).

RESULTS

Tests of X Inactivation Potential. The competence of the *Xic* deletion clones to carry out different steps of X inactivation was tested in the following ways. (*i*) Counting was suggested by dual expression of Tg and endogenous *Xist* RNA during differentiation, a time when *Xist* becomes repressed in male cells that do not undergo X inactivation. Persistent endogenous *Xist* expression implied that male cells sensed the presence of additional X chromosomes and could choose the X for inactivation (11). (*ii*) Initiation and establishment of X inactivation were assessed by the spread of *Xist* RNA along the chromosome in cis. (*iii*) Silencing and heterochromatin formation were assessed by delayed DNA replication timing and histone hypoacetylation. *A priori, Xic* defects could occur in some or all of these steps. Analysis of X inactivation potential showed that the deletions could be grouped into two classes. Only representative clones of each class are shown below. Tg lines derived from each *Xic* construct behaved similarly, with rare exception as noted below.

Class I. Class I clones also enacted X inactivation and included *Xist*-containing clones with 25–35 kb of flanking sequence on both sides. These are F7, F9, R3, R9, R42, F21, F47, πJL1, and πJL2.

***Xist* Expression, Chromosome Counting, and Choice in Class I Clones.** X inactivation is induced in ES cells by differentiation

into embryoid bodies (EB) in culture (24, 25). In both undifferentiated male and female ES cells, *Xist* is expressed at low levels and can be visualized by FISH as a pinpoint signal localized to the *Xic* (2). Differentiation in male cells represses *Xist* expression (Fig. 2 *A* and *B*, J1). Differentiation in female cells leads to high expression and spread of *Xist* RNA over the future X_i and repression of *Xist* from the active X. This developmentally regulated *Xist* expression is recapitulated in 116.6, an ES line carrying ≈20 copies of the 450-kb Y116 Tg (Fig. 2 *A* and *B*), where differentiation results in choosing between the X and autosome for inactivation (11).

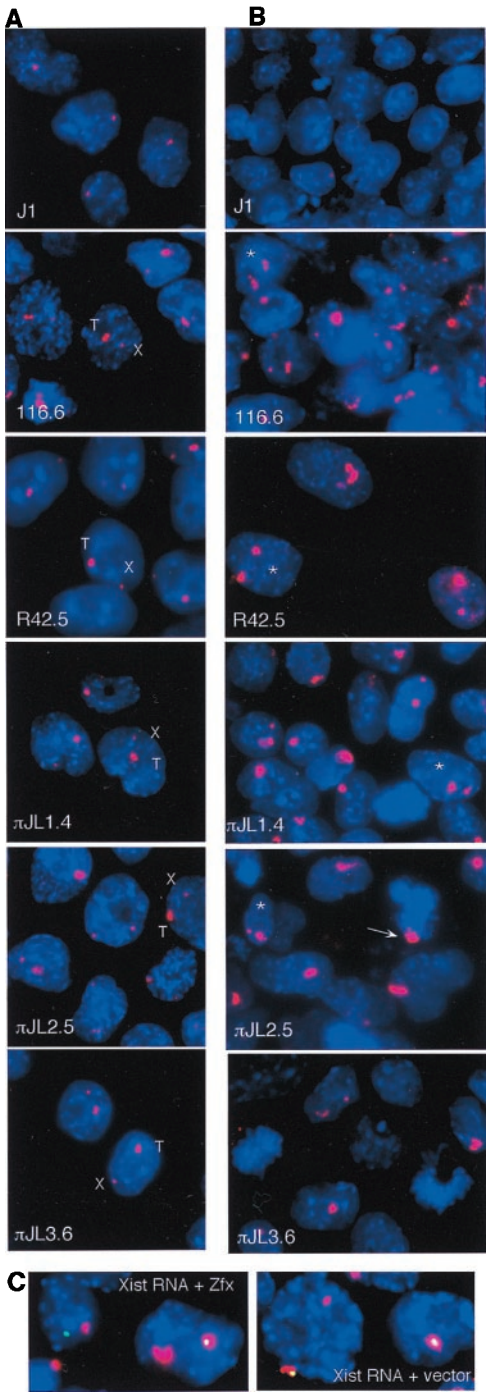

FIG. 2. *Xist* expression in Tg ES and EB cells. (*A*) RNA FISH of undifferentiated ES cells with a rhodamine-labeled *Xist* probe (red). X, endogenous; T, Tg; Blue, 4′,6-diamidino-2-phenylindole (dapi) staining. (*B*) RNA FISH of day 9 EB cells (*Xist* RNA, red). Double *Xist* expressers are indicated by asterisks; the arrow indicates *Xist* RNA coat on a πJL2.5 metaphase chromosome. (*C*) RNA/DNA FISH for *Xist* RNA (red) and *Zfx* or vector DNA (FITC, green) was performed for all ES lines to determine *Xist* RNA origin. πJL2.5 EB is shown. Coincident red and green resulted in white.

The ability of the *Xic* deletion clones to enact *Xist* expression and chromosome counting was analyzed by RNA FISH. Fig. 2*A* depicts *Xist* RNA patterns in undifferentiated ES cells. In the undifferentiated state, all Tg lines showed *Xist* expression from endogenous and ectopic loci. RNA/DNA FISH (not shown) indicated that *Xist* could be expressed from either the X or autosome. As in 116.6, the autosomal *Xist* signals were reproducibly larger and more intense than the endogenous *Xist* signals. The signal size directly reflected Tg copy number, consistent with expression from multiple Tg copies.

Differentiation of class I clones showed that they behaved like 116.6 Tg. At a time when J1 and N1.1 cells have lost *Xist* expression, class I Tg cells showed high *Xist* expression and transcripts that coated the autosome (Fig. 2*B*). *Xist* RNA was observed in 65–100% of all EB cells (Table 2). Consistent with previous observations in 116.6 EB (11), cultures contained both single expressers with only Tg RNA and double expressers with both Tg and endogenous transcripts (Fig. 2 *B* and *C*; Table 2). The Tg RNA cluster was large, whereas the endogenous cluster varied in size (though it was usually smaller than Tg RNA). The smaller size of the endogenous cluster may reflect incomplete ES differentiation or selection against cells that have spread *Xist* RNA along the X.

The persistent expression of endogenous X*ist* can be explained in one of two ways. First, the introduction of multiple X*ic* transgenes may titrate out factors required to repress X*ist*. Alternatively, the ability to express both endogenous and Tg *Xist* may reflect the presence of a counting element on the Tg as previously hypothesized (11). In this case, double expressors would account for the majority because each tandem X*ic* Tg is recognized as a different X chromosome and that the rules of counting require all but one X to express *Xist* and undergo inactivation. Thus, a Tg clone with four *Xic* insertions would have simultaneous autosomal and X linked *Xist* expression in four of five cells. Although double expressers generally accounted for the majority of day 9 EB cells, there was not a direct correlation between Tg copy number and percentage of double expression (Table 2). This lack of correlation may be caused by continuous loss of double expressers as a result of X inactivation. Indeed, increased cell death was seen for class I clones compared with J1 and N1.1 (data not shown), consistent with inactivation of important X linked or autosomal genes during differentiation.

Table 2. Pattern of *Xist* expression in Tg EB cells

ES line	Double expressors, %	Single expressors, %		*Xist*-expressing cells in day 9 EB cultures, %
	Endogenous + Tg	Endogenous only	Tg only	
F7.26	65	0	35	100
F9.18	60	0	40	100
R3.6	50	0	50	65
R9.11	75	0	25	100
F21.21	60	0	40	80
F47.2	55	0	45	75
R42.19	80	0	20	100
πJL1.4	35	0	65	90
πJL2.4	50	0	50	80
πJL3.10	20	0	80	30
116.6	45	0	55	90
N1.1	—	—	—	10
J1	—	—	—	<10

The right column indicates the percentage of *Xist*-expressing cells in the entire day 9 EB culture. Numbers in column 2, 3, and 4 are the percentages of double or single expressers of all *Xist*-expressing cells. Percentages are rounded off to nearest fifth percentile and were gathered in three experiments ($n > 200$ nuclei for each experiment).

Therefore, the number of double expressers counted on day 9 likely reflected only a fraction of the total.

Somatic *Xist* Expression in Class I Clones: The RNA Skips the *Xic*. Fibroblasts were isolated from chimeric Tg mice to determine whether *Xist* expression was maintained in somatic cells and was accompanied by chromosome inactivation; five independently cloned fibroblast lines for each ES line were examined by RNA FISH (fibroblasts were denoted by an additional number following the ES designation; e.g., πJL2.5.5 was derived from ES πJL2.5). Because cells were immortalized by simian virus 40-large T antigen, each fibroblast clone consisted of diploid and polyploid cells. All showed abundant, highly localized *Xist* RNA transcripts (Fig. 3*A*; $n > 2{,}000$; >95% of nuclei have *Xist* signals). As for 116.6 somatic cells, *Xist* was expressed exclusively from the Tg locus and never from the X. This result is consistent with selection against cells expressing endogenous *Xist* because of deficiency of X linked gene expression. As in female and 116.6 somatic cells, expression of *Xist* RNA resulted in coating of the chromosome in cis by *Xist* RNA. A chromosome-wide coat could be found in >95% of cells in prophase, 40–80% of those in metaphase, and 0% of anaphase cells ($n > 100$ for each; data not shown). The spread of the Tg-derived RNA was cis-limited (Fig. 3*B*) with two exceptions. The centromere was skipped on all Tg autosomes as on the female X_i. The Tg themselves were devoid of coating in clones carrying only 80 kb of *Xic* sequence (Fig. 3*C*). As shown by DNA hybridization with Tg probes, the skip occurred at the Tg.

DNA Replication Timing in Class I Clones. The X_i replicates late in S phase (4). The Tg autosome of 116.6 also exhibited delayed replication timing (12). To determine whether this property was retained in the deletion derivatives, we examined replication timing in Tg fibroblasts by differential incorporation of BrdUrd into euchromatic and heterochromatic regions. BrdUrd was added to cell cultures during late S phase, and metaphase chromosomes were prepared after a 6-h incubation. When performed on normal fibroblast lines, this procedure labeled the X_i in female cells and the Y in male cells, both of which have been established as late-replicating chromosomes (26). In class I lines, the Y and Tg autosome were consistently and diffusely labeled by BrdUrd (Fig. 4). In πJL1.3.3, 35 of 48 metaphases showed colabeling of the Ch13 Tg and the Y, whereas 13 of 48 showed labeling only of the Y. In πJL1.4.1, 42 of 45 showed colabeling of both the Ch3 Tg and the Y, whereas 3 of 45 showed labeling of only the Y. In πJL2.5.5, 31 of 40 showed colabeling of the Ch8 Tg and the Y, whereas 9 of 40 showed labeling of only the Y. The consistent labeling of the Y confirmed that we had examined BrdUrd incorporation in late S phase. Thus, these observations indicated that class I sequences induced late replication. The labeling of Tg autosomes varied. In some, the entire autosome was labeled diffusely. In others, regions closest to the Tg were labeled more brightly, suggesting a distance-dependent influence of the autosomally placed *Xic* on DNA replication. On average, the BrdUrd density on autosomes was less than that for the X_i and Y, suggesting that regions of early replication were interspersed with late-replicating regions. Isolated loci of other chromosomes also were labeled, possibly representing focal heterochromatin.

H4 Hypoacetylation in Class I Clones. X inactivation has been associated with panchromosomal histone hypoacetylation (Fig. 5*C*; ref. 5). We previously showed that autosome silencing by the *Xic* also is correlated with H4 hypoacetylation (12). Here, we tested whether *Xic* deletion clones retained the ability to induce hypoacetylation. Immunofluorescence with antiacetylated H4 antibodies showed that all class I Tg induced histone deacetylation. In a representative class I clone shown in Fig. 5*A*, the Ch8 Tg and the Y were hypoacetylated consistently for πJL2.5.5 ($n = 33$). As on the X_i, hypoacetylation extended bidirectionally from centromere to telomere. Furthermore, like the X_i, the Tg chromosomes reproducibly displayed one to three islands of acetylation, suggesting that sporadic gene clusters escaped heterochromatinization (12). These islands occurred most frequently at the Tg and at distal regions. πJL1.4.1 showed two patterns of hypoacetylation (Fig. 5*B*; $n = 51$). In 23 of 51 chromosome spreads, H4 acetylation was low throughout the Ch3 Tg. However, in 28 of 51 spreads, H4 immunofluorescence indicated that acetylation was low on the proximal half of the Ch3 Tg but was higher on the distal half.

Class II. πJL3-derived class II clones expressed Tg *Xist* in undifferentiated cells but are defective for X inactivation in somatic cells. πJL3 carried the P_1 promoter of *Xist* but lacks P_0 sequences (19).

***Xist* Expression, Chromosome Counting, and Choice in Class II Mutants.** In the undifferentiated state, Tg ES cells derived from πJL3 showed Tg *Xist* expression despite the fact that they lacked the P_0 promoter (Fig. 2*A*). Thus, P_0 is not required absolutely for ES cell *Xist* expression, a result consistent with a prior observation that P_1 can act as a minimal *Xist* promoter in ES cells (27–29). During EB differentiation, *Xist* expression persisted in a minority of cells in five independent lines (πJL3.1, πJL3.6,

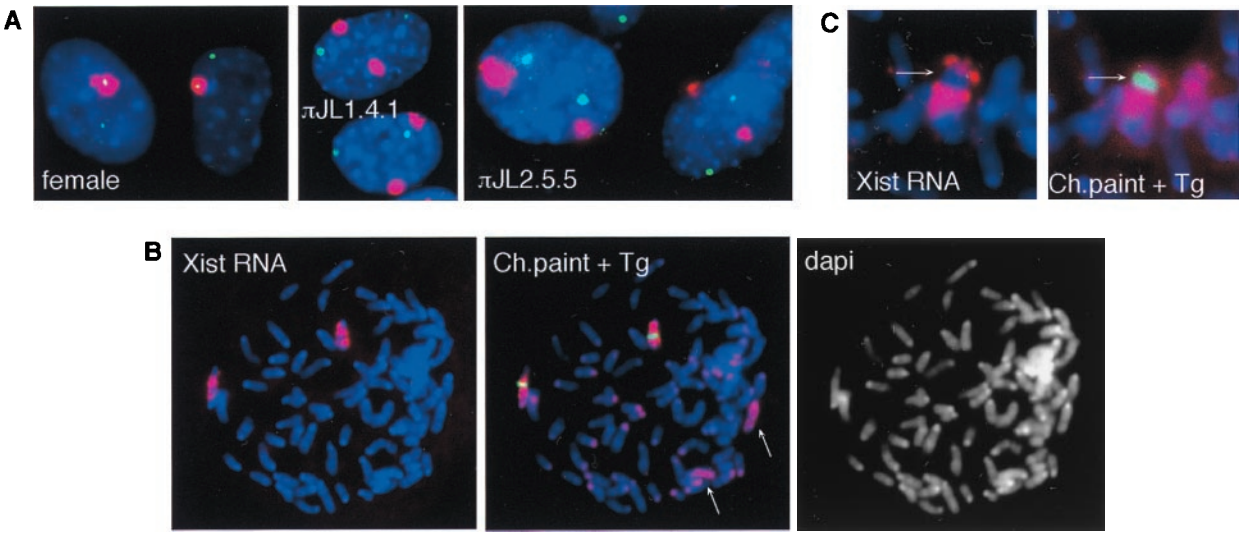

FIG. 3. *Xist* is expressed in class I somatic cells, and the RNA coats the autosome. (*A*) RNA/DNA FISH of normal female and Tg fibroblasts. *Xist* RNA is shown in red; *Zfx* genomic DNA is shown in green. (*B*) πJL1.4.1 chromosomes were hybridized to *Xist* probes (red) without chromosome denaturation, then stripped, denatured, and hybridized to chromosome 3 (Ch3)-specific paints (Ch.paint; red) and Tg probes (green). Arrows indicate normal homologues of Ch3. (*C*) *Xist* RNA skips the *Xic* Tg as indicated by the arrows. This experiment was performed as described for *B*.

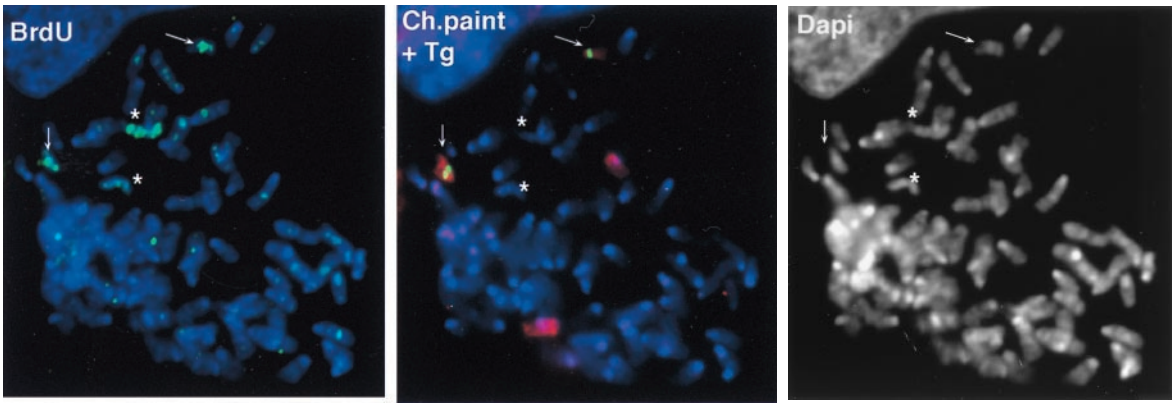

FIG. 4. Delayed replication timing of the Tg autosome in class I fibroblasts. πJL2.5.5 is shown. Arrows indicate labeling by Ch8-specific paints (Ch.paint) and Tg probes; asterisks indicate Y. BrdU, BrdUrd.

πJL3.8, πJL3.9, and πJL3.10; Fig. 2*B*; Table 2). Loss of expression was unlikely to be caused by position effects, as the five lines have different insertion sites. Interestingly, fewer double expressers were seen in class II lines than in class I Tg (Table 2). These results are consistent with either the loss of a counting element in πJL3 or the deletion of a transcriptional regulator separate from chromosome counting.

Class II Mutants Are Defective in Somatic *Xist* Expression. In contrast to class I clones, class II fibroblasts from πJL3.6, πJL3.8, πJL3.9, and πJL3.10 did not show any *Xist* expression. Thus, somatic *Xist* expression was compromised in class II clones despite apparently normal expression in ES cells. Together with prior studies (19, 27, 29), these results suggested that separate genetic elements control *Xist* expression in undifferentiated ES and somatic cells.

Class II Mutants Are Defective in Heterochromatin Formation. The BrdUrd assay showed that the Tg autosomes of class II clones were not grossly late-replicating. In over 50 metaphases examined for fibroblasts derived from πJL3.6, πJL3.8, and πJL3.10, not one showed diffuse BrdUrd incorporation, whereas nearly all had a brightly stained Y (not shown). Immunofluorescence with antiacetylated H4 antibodies also indicated that fibroblasts from πJL3.6, πJL3.8, and πJL3.10 could not induce H4 hypoacetylation. Although the Y was hypoacetylated consistently, not one Tg chromosome was grossly hypoacetylated (not shown). Thus, πJL3 lacked the sequences to induce late replication and H4 hypoacetylation.

Survival of Mouse Chimeras. The results presented above suggest that class I deletions retain all important *Xic* elements, whereas the class II deletion removes essential sequences for the expression of *Xist* during differentiation and in somatic cells. This conclusion is supported by the reduced viability *in vivo* of class I relative to class II cells. Chimeric animals were generated easily by class II ES cells despite a high percentage chimerism (70–90%). No phenotype was seen even when the Tg was inserted into the X (πJL3.8). In contrast, class I chimeras were difficult to generate, with most pups dying *in utero*. In a πJL1.3 chimera, a sixth postaxial digit was evident in the posterior limbs. This extra digit was interesting in light of the fact that the insertion occurred near the telomere of Ch13. The *extra toes* locus (*Xt*; *Gli3*) maps near the centromere of Ch13 and was identified in a mouse with six toes carrying an 80-kb deletion on one allele (30). This identification raises the interesting possibility that the phenotype in πJL1.3 resulted from long-range silencing of the *Xt* locus.

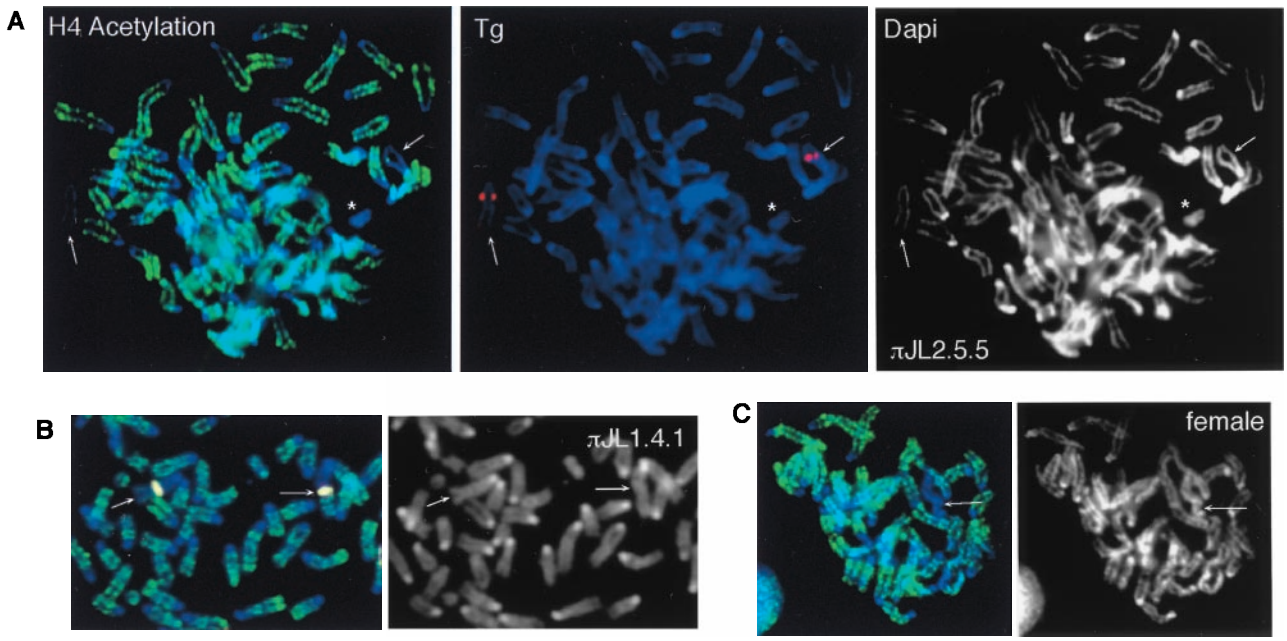

FIG. 5. H4 hypoacetylation of Tg autosomes in class I somatic cells. (*A*) Immunofluorescence of πJL2.5.5 chromosome spreads with antiacetylated H4 antibodies (green). The Ch8 Tg (arrows) and the Y (asterisk) were hypoacetylated. The Tg is shown in red. (*B*) In πJL1.4.1, some Tg autosomes showed partial deacetylation (arrows). The Tg is pseudocolored yellow. (*C*) A control female cell showing one hypoacetylated X_i (arrow).

DISCUSSION

We have created large-scale deletions of the murine *Xic* and analyzed their effects on X inactivation by using Tg-based assays. The class I deletions showed that more than 80% of the previously defined *Xic* interval could be removed without obvious effects on initiation, spread, and establishment of cis inactivation. Only an 80-kb domain is required, a region that includes the *Xist* gene and approximately 30 kb of upstream and 30 kb of downstream sequence. This region includes the 35-kb cosmid sequence identified by Herzing *et al.* (13).

Our work supports the feasibility of using a Tg approach in studying X inactivation. Because multiple cell lines with different insertion sites were examined for each deletion, this study suggests that long-range cis effects of the 80-kb region can be generalized to many autosomes. Indeed, the *Xic* Tg could overcome position effects, which had been invoked to explain why other *Xic* Tg studies had not found cis inactivation of autosomes (31, 32). The different outcomes may be explained by other factors, such as the method used to create Tg lines or Tg copy number. The idea that a high copy number increases *Xic* efficacy is an interesting one that warrants further investigation.

The data strengthen the hypothesis that the *Xic* works in a context-independent manner (12). This hypothesis is consistent with the behavior of X-to-autosome translocation chromosomes on which silencing can spread into the autosomal segment (33–35). It has been postulated that its long-range influence is enhanced by "way stations" (36), cis elements that reinforce the inactivation signal as it travels outwards from the *Xic*. These cis elements may be specific *Xist* RNA-binding sites. If way stations exist on the X chromosome, related sequences must also occur on autosomes. Such way stations are likely to be qualitatively different from those on the X. Although long-range effects were reproducible among class I Tg, differences from X inactivation were seen with regard to the extent of late DNA replication on the Tg autosome, suggesting that autosomal inactivation is less complete or stable.

The observation that Tg *Xist* RNA skips the ectopic *Xic* raises the possibility that the *Xic* lacks *Xist*-binding sites and therefore escapes inactivation on the X_i. Interestingly, skipping could be observed only on chromosomes carrying 80-kb P1 Tg and was not evident on those carrying larger YAC inserts (e.g., 116.6). This difference is perhaps because larger Tg carry non-*Xic* sequences that undergo X inactivation and might be expected to bind *Xist* RNA, thereby resulting in perceived coating of the Tg. Because a skip is not seen at the endogenous *Xic,* we believe that the combination of having multicopy *Xic* insertion and having only the minimal 80-kb *Xic* sequence enabled us to see the skip region in class I P1 Tg. These observations also raise the possibility that other X linked genes might escape X inactivation by a similar mechanism.

Analysis of class II clones showed that ES cell *Xist* expression can be separated from later events of X inactivation and that removal of 5′ *Xist* sequences abolished cis inactivation. Together with other studies (19, 27, 29), our data implicate 5′ sequences in controlling *Xist* expression. It has been proposed that developmentally specific *Xist* regulation requires an ES-specific promoter (P_0) located 6 kb upstream of P_1 and that the switch from P_0 to P_1 enables high *Xist* expression (19). Because πJL3 lacks P_0 sequences but still expresses *Xist* in ES cells, P_0 is not required absolutely for *Xist* expression in ES cells. This finding is consistent with prior studies that showed that P_1 alone can function as a minimal promoter in both ES and somatic cells (27–29). In the context of other published work, our study also suggests important elements downstream of *Xist*. It has been proposed that a counting element or repressor of *Xist* resides in a 65-kb region downstream of *Xist* (16). Because the 80-kb *Xic* region identified by our study extends only 30 kb downstream, the combined evidence suggests that the *Xist* regulator resides in the 30-kb region.

This work shows that somatic X inactivation can be recapitulated by an 80-kb multifunctional domain. By showing that long-range cis effects can be generalized to many autosomes, we have established that Tg-based models for X inactivation serve as reasonable alternatives to mouse knockouts. Future studies will address whether this region is also sufficient for other forms of X inactivation, such as imprinted and male germ-line X inactivation (37, 38). The reduction to 80 kb now makes a detailed and comprehensive mutagenesis of the *Xic* to identify specific regulatory sequences more feasible.

We thank B. Seed for use of the mouse facility, and J. E. Kirby, B. Migeon, N. Stavropoulos, D. Warshawsky, and Y. Ogawa for critical reading of the manuscript. This work was funded by American Cancer Society Award ACS-IRG173H and a Hoechst award to J.T.L.

1. Lyon, M. F. (1961) *Nature (London)* **190,** 372–373.
2. Lee, J. T. & Jaenisch, R. (1997) *Curr. Opin. Genet. Dev.* **7,** 274–280.
3. Mohandas, T., Sparkes, R. S. & Shapiro, L. J. (1981) *Science* **211,** 393–396.
4. Priest, J. H., Heady, J. E. & Priest, R. E. (1967) *J. Cell Biol.* **35,** 483–487.
5. Jeppesen, P. & Turner, B. M. (1993) *Cell* **74,** 281–289.
6. Rastan, S. & Brown, S. D. M. (1990) *Genet. Res.* **56,** 99–106.
7. Brown, C. J., Ballabio, A., Rupert, J. L., Lafreniere, R. G., Grompe, M., Tonlorenzi, R. & Willard, H. (1991) *Nature (London)* **349,** 38–44.
8. Clemson, C. M., McNeil, J. A., Willard, H. & Lawrence, J. B. (1996) *J. Cell Biol.* **132,** 259–275.
9. Penny, G. D., Kay, G. F., Sheardown, S. A., Rastan, S. & Brockdorff, N. (1996) *Nature (London)* **379,** 131–137.
10. Rastan, S. & Robertson, E. J. (1985) *J. Embryol. Exp. Morphol.* **90,** 379–388.
11. Lee, J. T., Strauss, W. M., Dausman, J. A. & Jaenisch, R. (1996) *Cell* **86,** 83–94.
12. Lee, J. T. & Jaenisch, R. (1997) *Nature (London)* **386,** 275–279.
13. Herzing, L. B. K., Romer, J. T., Horn, J. M. & Ashworth, A. (1997) *Nature (London)* **386,** 272–275.
14. Brockdorff, N. (1998) *Curr. Opin. Genet. Dev.* **8,** 328–333.
15. Marahrens, Y., Panning, B., Dausman, J., Strauss, W. & Jaenisch, R. (1997) *Genes Dev.* **11,** 156–166.
16. Clerc, P. & Avner, P. (1998) *Nat. Genet.* **19,** 249–253.
17. Pavan, W. J., Hieter, P. & Reeves, R. H. (1990) *Proc. Natl. Acad. Sci. USA* **85,** 6027–6031.
18. Kusumi, K., Smith, J. S., Segre, J. A., Koos, D. S. & Lander, E. S. (1993) *Mamm. Genome* **4,** 391–392.
19. Johnston, C. M., Nesterova, T. B., Formstone, E. J., Newall, A. E. T., Duthie, S. M., Sheardown, S. A. & Brockdorff, N. (1998) *Cell* **94,** 809–817.
20. Li, E., Bestor, T. H. & Jaenisch, R. (1992) *Cell* **69,** 915–926.
21. Lee, J. T. & Jaenisch, R. (1996) *Nucleic Acids Res.* **24,** 5054–5055.
22. Lawrence, J. B., Singer, R. H. & Marselle, L. M. (1989) *Cell* **57,** 493–502.
23. Trask, B. J. (1991) *Trends Genet.* **7,** 149–154.
24. Martin, G. R., Epstein, C. J., Travis, B., Tucker, G., Yatziv, S., David, W., Martin, J., Clift, S. & Cohen, S. (1978) *Nature (London)* **271,** 329–333.
25. Kay, G. F., Penny, G. D., Patel, D., Ashworth, A., Brockdorff, N. & Rastan, S. (1993) *Cell* **72,** 171–182.
26. Schempp, W. (1985) in *The Y Chromosome*, ed. Sandberg, A. A. (Liss, New York), pp. 357–371.
27. Hendrich, B. D., Plenge, R. M. & Willard, H. F. (1997) *Nucleic Acids Res.* **25,** 2661–2671.
28. Pillet, N., Bonny, C. & Schorderet, D. F. (1995) *Proc. Natl. Acad. Sci. USA* **92,** 12515–12519.
29. Sheardown, S. A., Newall, A. E. T., Norris, D. P., Rastan, S. & Brockdorff, N. (1997) *Gene* **203,** 159–168.
30. Lyon, M. F., Rastan, S. & Brown, S. D. M. (1996) *Genetic Variations and Strains of the Laboratory Mouse* (Oxford Univ. Press, Oxford).
31. Heard, E., Dress, C., Mongelard, F., Courtier, B., Rougeulle, C., Ashworth, A., Vourch, C., Babinet, C. & Avner, P. (1996) *Hum. Mol. Genet.* **5,** 441–450.
32. Matsuura, S., Episkopou, V., Hamvas, R. & Brown, S. D. M. (1996) *Hum. Mol. Genet.* **5,** 451–459.
33. Keitges, E. A. & Palmer, C. G. (1986) *Hum. Genet.* **72,** 230–236.
34. Eicher, E. M. (1970) *Adv. Genet.* **15,** 175–259.
35. White, W. M., Willard, H. F., Dyke, D. L. V. & Wolff, D. J. (1998) *Am. J. Hum. Genet.* **63,** 20–28.
36. Gartler, S. M. & Riggs, A. D. (1983) *Annu. Rev. Genet.* **17,** 155–190.
37. Richardson, B. J., Czuppon, A. B. & Sharman, G. B. (1971) *Nat. New Biol.* **230,** 154–155.
38. Monesi, V. (1965) *Exp. Cell Res.* **39,** 197–224.